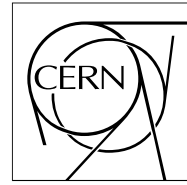


The Compact Muon Solenoid Experiment

CMS Note

Mailing address: CMS CERN, CH-1211 GENEVA 23, Switzerland



December 3, 1997

Impact of Fast Shaping at the Front-end on Signals from Micro Strip Gas Chambers

F. G. Sciacca

Imperial College of Science, Technology & Medicine, London, UK

Abstract

The ballistic deficit due to fast shaping time constants at the front-end amplifier is evaluated using Monte Carlo generated events simulating isolated hits in MSGCs of CMS performance. The effect of the track incidence angle is also investigated up to 45 degrees.

1 Introduction

The problem of Bunch Crossing Interval (BCI) identification at LHC with tracking detectors which have long collection times, like MSGCs, has been widely studied in the past [1-4]. The precision of BCI identification improves when using shorter shaping time constants at the front-end amplifier. On the other hand, using shaping times shorter than the intrinsic charge collection time of the detector, or comparable with it, will result in a poor charge integration efficiency. The inefficiency is referred to as ballistic deficit.

The two effects are in direct contrast and the optimal choices for a given track reconstruction efficiency effectively depends on several parameters. One of them is the Signal to Noise ratio (S/N) achieved in the system, which is directly affected by the choice of the shaping time at the front-end amplifier: shorter shaping times will result in higher noise for the APV CMOS front-end amplifier, and higher ballistic deficit, thus contributing to a global deterioration of the S/N.

It is therefore important to try to characterize the effect in order to be able to predict and understand the implications of choosing the optimal shaping time at the front-end for a good BCI identification precision.

2 Data Used and Analysis Procedure

The analysis was performed on 10 sets of Monte Carlo generated events of MIPs in MSGCs whose performance is the one anticipated for the detectors which will be used in CMS tracker (table 1). Each set includes 5000 single hit events simulating isolated tracks entering the detector at angles of 0-45 degrees in 10 steps (1 set for each angle). The Monte Carlo program was developed at Pisa [5].

Table 1: MSGC parameters for the Monte Carlo simulation

gas thickness	3 mm
gas mix	Ne/Dme (33/77)
avg. n. of clusters	14
avg. n. of e-ion pairs	40
avg. gain	~2000
anode (readout)	gnd
cathode	-550 V
drift	-3.5 kV

The signal is generated according to the following method: a detector cell is defined which extends 100 μm both sides of the anode strip for the whole thickness of the detector as shown in figure 1. The particles enter the detector from the drift cathode in a random point within a window of $200 \mu\text{m} + 3 \cdot \tan\theta$ mm, θ being the incidence angle. Along the track they generate e-ion pairs, which undergo drift and diffusion. Only the charge which reaches the multiplication region while still remaining within the 200 μm width of the cell is multiplied and reaches the anode. Figure 2 shows the spectrum of the collected charge for normal incidence.

The signal, which at this stage is stored on disk in numerical form (current vs time) and does not include noise, is convoluted with an ideal CR-RC filter, whose temporal response is described by the following expression:

$$V(t) = G * (t / \tau) * \exp(-t / \tau) \text{ with } G \text{ representing an arbitrary gain factor.}$$

Four time constants τ are used in this simulation: 25, 40, 50 and 1000 ns. Figure 3 shows the pulse shapes obtained for one randomly chosen event. For each of the events and for each τ the peak value of the pulse after the shaping ($\text{peak}(\tau)$) and the peaking time are recorded. The ballistic deficit for each τ ($\text{BD}(\tau)$) is calculated according to the following formula:

$$\text{BD}(\tau) = [\text{peak}(1000) - \text{peak}(\tau)] / \text{peak}(1000)^1.$$

¹ This is an approximation, the correct formula being $\text{BD}(\tau) = [\text{peak}(\infty) - \text{peak}(\tau)] / \text{peak}(\infty)$. The uncertainty introduced is estimated to be less than 0.5%

The distributions of ballistic deficit and peaking time obtained for each of the time constants are fitted to Gaussians in order to estimate average values and dispersions.

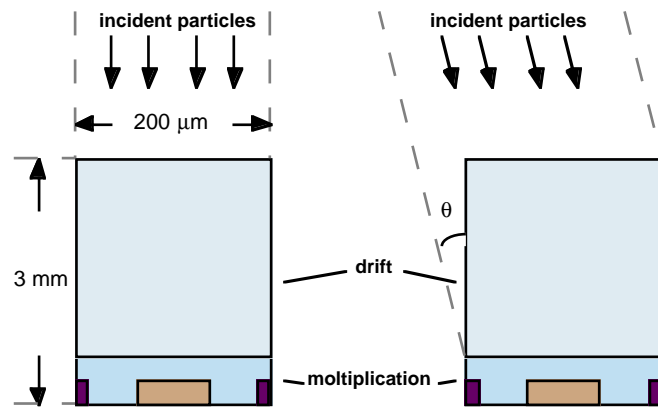


Figure 1: The detector cell defined for simulation purposes.

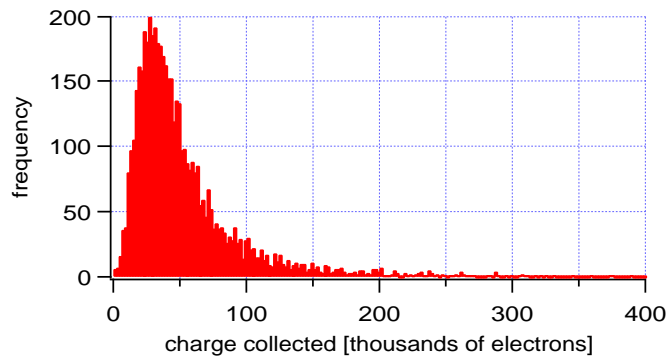


Figure 2: The spectrum of the charge collected in the detector cell defined above.

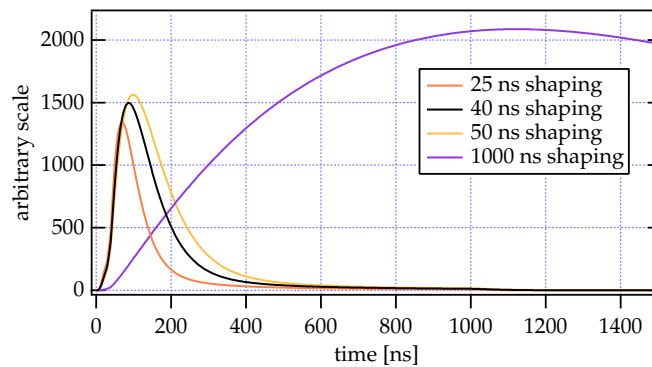


Figure 3: Typical pulse shape for different time constants: one event.

3 Results

3.1 Normal Incidence

Figure 4 illustrates the deterioration of the pulse height spectra at shorter shaping times. Figure 5 shows the distribution of peaking times after shaping and table 2 summarizes the values yielded by Gaussian fits. The distributions of ballistic deficit are shown in figure 6 and the average and dispersion values again in table 2.

In order to attempt an empirical parametrization of the effect I repeated the study using a larger range of time constants: 25, 40, 50, 200, 400, 600, 800, 900, 1000, 1100 ns and 1200 ns as normalization. The results are shown in figure 7. A fit to a double exponential yields the following expression:

$$BD(\tau) = 0.5 * \exp(-0.02*\tau) + 0.5 * \exp(-0.05*\tau).$$

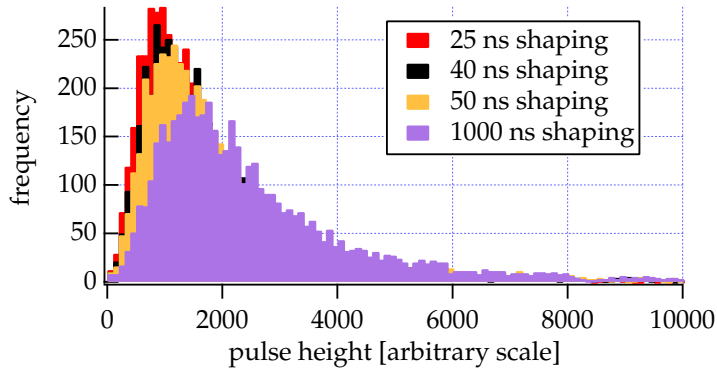


Figure 4: Pulse height distributions for the different shaping time constant

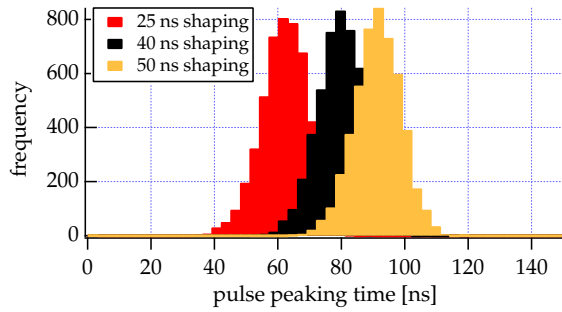


Figure 5: Pulse peaking time distributions.

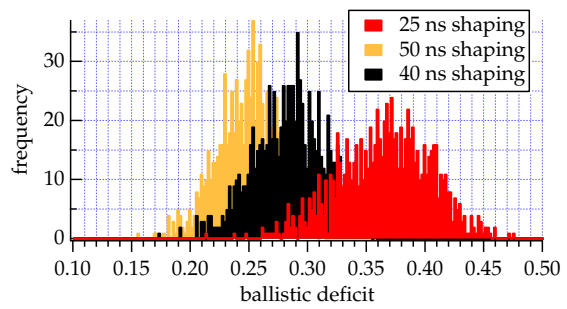


Figure 6: Ballistic deficit distribution

Table 2: Summary of average b. deficit and peak time values and their errors

time constant [ns]	avg. b. deficit %	sigma %	avg. peak. time [ns]	sigma [ns]
25	36.7	4	61	7.1
40	28.5	3	78	7.1
50	25.1	2.8	90	7.2
1000	-	-	1110	12.1

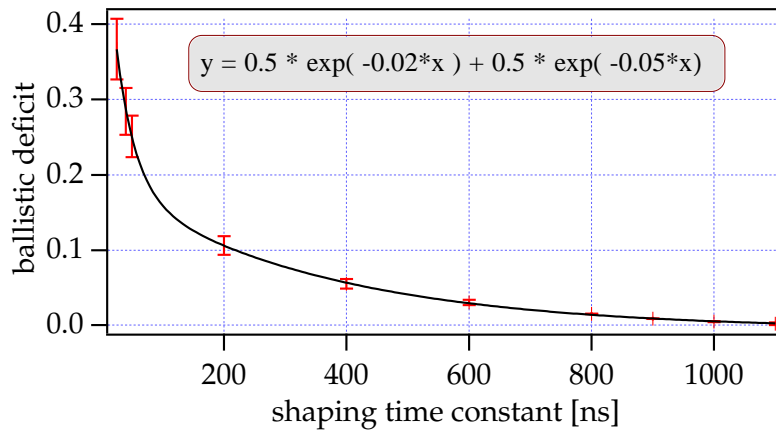


Figure 7: Ballistic deficit vs shaping time constant for a larger range of time constants

3.2 Inclined Tracks

Figure 8 shows that the average peaking time exhibits almost no dependence on incidence angle for each of the time constants. This is important because it will allow to preserve hit efficiency even at large angles, specially when further processing is performed on the analogue signal, such as in the case of deconvolution.

The average values of ballistic deficit at each shaping time as a function of the incidence angle are shown in figure 9. There is a slight increase in the values with increasing angle. This is contained within 3% for $\tau = 40$ and 50 ns and it seems to flatten out for angles > 20 degrees. With $\tau = 25$ ns the increase is around 1%.

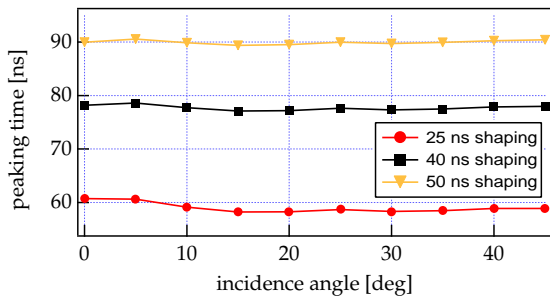


Figure 8: Pulse peaking time vs incidence angle

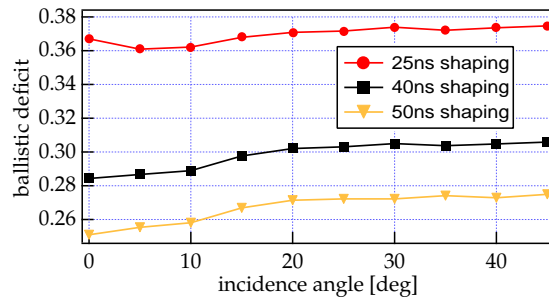


Figure 9: Ballistic deficit vs incidence angle

4 Conclusions

The impact of fast CR-RC shaping at the front end on signals from MSGC of CMS performance has been characterized for tracks of normal incidence and inclined up to 45 degrees.

Average peaking times of the shaped pulses are 61 ns for $\tau = 25$ ns, 78 ns for $\tau = 40$ ns and 90 ns for $\tau = 50$ ns. The ballistic deficit has been estimated to be 37% for $\tau = 25$ ns, 29% for $\tau = 40$ ns and 25% for $\tau = 50$ ns, with a typical error of about 4%. Shorter shaping times incur the penalty of increased noise: 10% effect going from 50 to 40 ns, 40% effect going from 50 to 25.

The effect of the angle of incidence on the average peaking times is negligible for each of the time constants. The effect on ballistic deficit is contained within a 3% increase with increasing angle.

Acknowledgments

I would like to thank Mario Spezziga at INFN Pisa for kindly providing the simulated events.

References

- [1] CMS TN/94-215, R. Sachdeva, “Signal Processing for MSGCs at CMS”
- [2] CMS NOTE/97-013, J.F. Clergeau et al., “Proposal for the Read-out Electronics of Gas Micro Strip Detectors in the CMS Tracker”
- [3] CMS NOTE/97-022, F. G. Sciacca “Study of Analogue Signal Processing Algorithms for MSGC Signals in CMS”
- [4] CMS IN/97-021, F. G. Sciacca “Definition of the Front-end Signal Processing Algorithm for MSGCs in CMS”
- [5] INFN PI/AE-94-02 (1994), R. Bellazzini, M.A. Spezziga, “Electric Field, Avalanche Growth and Signal Development in Micro-Strip Gas Chambers and Micro-Gap Chambers”